Research Article

Journal of PeptideScience

Received: 15 July 2010 Revised: 2 September 2010 Accepted: 2 September 2010 Published online in Wiley Online Library: 26 October 2010

(wileyonlinelibrary.com) DOI 10.1002/psc.1308

Nanoparticles containing octreotide peptides and gadolinium complexes for MRI applications‡

Antonella Accardo,[a] Anna Morisco,[a] Eliana Gianolio,[b] Diego Tesauro,[a] Gaetano Mangiapia,[c] Aurel Radulescu,[d] Astrid Brandt[e] and Giancarlo Morelli[a]*

New mixed nanoparticles were obtained by self-aggregation of two amphiplic monomers. The first monomer $(C18)_2$L5-Oct contains two C18 hydrophobic moieties bound to the *N*-terminus of the cyclic peptide octreotide, and spaced from the bioactive peptide by five units of dioxoethylene linkers. The second monomer, $(C18)_2$DTPAGlu, $(C18)_2$DTPA or $(C18)_2$DOTA, and the corresponding Gd(III) complexes, contains two C18 hydrophobic moieties bound through a lysine residue to different polyamino-polycarboxy ligands: DTPAGlu, DTPA or DOTA. Mixed aggregates have been obtained and structurally characterized by small angle neutron scattering (SANS) techniques and for their relaxometric behavior. According to a decrease of negative charges in the surfactant head-group, a total or a partial micelle-to-vesicle transition is observed by passing from $(C18)_2$DTPAGlu to $(C18)_2$DOTA. The thicknesses of the bilayers are substantially constant, around 50 Å, in the analyzed systems. Moreover, the mixed aggregates, in which a small amount of amphiphilic octreotide monomer $(C18)_2$L5-Oct (10% mol/mol) was inserted, do not differ significantly from the respective self-assembled systems. Fluorescence emission of tryptophan residue at 340 nm indicates low mobility of water molecules at the peptide surface. The proton relaxivity of mixed aggregates based on $(C18)_2$DTPAGlu(Gd), $(C18)_2$DTPA(Gd) and $(C18)_2$DOTA(Gd) resulted to be 17.6, 15.2 and 10.0 mM^{-1} s^{-1} (at 20 MHz and 298K), respectively. The decrease in the relaxivity values can be ascribed to the increase in τ_M (81, 205 and 750 ns). The presence of amphiphilic octreotide monomer exposed on mixed aggregate surface gives the entire nanoparticles a potential binding selectivity toward somatostatin sstr2 receptor subtype, and these systems could act as MRI target-specific contrast agent. Copyright © 2010 European Peptide Society and John Wiley & Sons, Ltd.

Keywords: amphiphilic gadolinium complexes; octreotide peptide; MRI contrast agents; supramolecular aggregates; small-angle neutron scattering

Introduction

Regulatory peptides represent a group of different families of molecules known to act on multiple targets in the human body at extremely low concentrations. They control and modulate the function of almost all key organs and metabolic processes, acting on several targets such as the brain; the gastrointestinal tract; the endocrine system; the kidneys; the lungs, and the immune, vascular, and peripheral nervous systems. Their action is mediated through specific membrane receptors; almost all belonging to the group of G protein-coupled receptors [1,2].

Several synthetic analogs or chemically stabilized derivatives of these peptides are studied as therapeutic agents in several pathologies. The most successful example is the somatostatin peptide: a cyclic 8-aa peptide (octreotide) (Sandostatin®, Novartis, Basel, Switzerland) [3]. This somatostatin analog is able to induce endocytosis by binding to SSTR2 with high (IC_{50} = 2 nM) and to SSTR 3 (IC_{50} = 376 nM) and SSTR 5 (IC_{50} = 299 nM) with low affinity [4]. Because of the presence of unnatural D-amino acid residues and the alcoholic *C*-terminus this peptide is highly resistant to enzymatic degradation and is able to restore the β-turn conformation required for interaction with the somatostatin receptors [5]. In the light of these properties and of the non-toxic side effects, octreotide is clearly a useful tool in cancer

* *Correspondence to: Giancarlo Morelli, Department of Biological Sciences, CIRPeB University of Naples "Federico II", Via Mezzocannone 16, 80134 Naples, Italy. E-mail: gmorelli@unina.it*

a *Department of Biological Sciences, CIRPeB, University of Naples "Federico II", & IBB CNR, Via Mezzocannone 16, 80134 Naples, Italy*

b *Department of Chemistry I.F.M. & Molecular Imaging Centre, University of Turin Via Nizza, 52, 10125 Turin, Italy*

c *Department of Chemistry, University of Naples "Federico II", Via Cinthia, 80126 Naples, Italy*

d *Juelich Centre for Neutron Science, Lichtenbergstrasse 1 D 85747 Garching, Germany*

e *Helmholtz Zentrum Berlin, Glienicker Strasse 100, D-14109 Berlin, Germany*

‡ *Special issue devoted to contributions presented at the E-MRS Symposium C "Peptide-based materials: from nanostructures to applications", 7–11 June 2010, Strasbourg, France.*

Abbreviations used: *DIEA, diisopropylethylamine; DMF, N,N-dimethylformamide; $(DOTA(tBu)_3$, (1,4,7,10-tetraazacyclododecane-1,4,7,10-tetraacetate tert-butyl ester); $DTPA(tBu)_4$ diethylenetriaminepentaacetate tetra-tert-butyl ester; $DTPAGlu(tBu)_5$, N,N-bis[2-[bis[2-(1,1-dimethyletoxy)-2-oxoethyl]-amino]ethyl]-L-glutamic acid 1-(1,1-dimethylethyl)ester; Fmoc-AdOO-OH,*

Journal of PeptideScience

management; indeed more than 10 years ago it was introduced in clinical practice to limit tumor growth [6]. Moreover, octreotide has been used to deliver therapeutics or diagnostics on the cellular target. In fact, by using the endocytosis mechanism [7] in which, after octreotide binding, the receptor-ligand complex is internalized, octreotide-drug conjugates containing the spindle poison taxol [8] and peptide nucleic acid (PNA) sequences as antisense therapeutics [9] have been developed. Furthermore, for diagnostic use several octreotide derivatives modified at the *N*-terminus with a bifunctional chelator suitable for labeling radiometals such as ^{99m}Tc, ^{111}In, and $^{67/68}$Ga have been designed, synthesized, and used as *in vivo* contrast agents in nuclear medicine techniques (SPECT and PET) [10–13].

The use of octreotide as target-selective delivery tool of therapeutic or diagnostic nanoparticles is a very challenging objective. Functionalized nanoparticles containing bioactive peptides exposed on their external surface have been proposed as target selective drug carriers [14,15], as target selective contrast agents in MRI [16–18], or as multimodal systems in which target selective therapeutic and imaging properties are combined [19,20].

MRI contrast agents based on nanoparticles (micelles or liposomes) have been developed with the aim of enhancing the contrast efficacy. The labeling of gadolinium containing micelles and liposomes with bioactive peptides combine the high relaxivity of the supramolecular aggregate and the target selectivity due to the presence of the bioactive peptide.

Recently, we developed several supramolecular aggregates derivatized with cholecystokinin (CCK8) [21–24] or bombesin (7-14-bombesin) peptide fragments [25] which act as target selective MRI contrast agents on cells overexpressing cholecystokininin and GRP receptors, respectively. Moreover, we reported the relaxometric behavior of novel paramagnetic micelles obtained by self-assembling of a monomer containing, in the same molecule, three different functions: (i) the chelating agent (DTPAGlu or DOTA) able to coordinate gadolinium ion, (ii) the octreotide bioactive peptide, and (iii) a hydrophobic moiety with two 18-carbon atoms alkyl chains [26]. The self-assembled DTPAGlu(Gd)octreotide micelles present high relaxivity values, high stability upon dilution, and efficient exposure of the bioactive octreotide peptide on the micelle external surface. Anyway, due to the simultaneous presence of an octreotide molecule and a gadolinium complex in each amphiphilic monomer the Gd/peptide ratio in the final aggregate is one and cannot be modified during nanoparticles formation. Thus, by increasing the number of paramagnetic gadolinium centers in the aggregate to enhance the relaxometric properties of the contrast agent, the number of peptide moieties on the aggregate surface also increases, providing peptide–peptide interactions that could prevent peptide–receptor binding.

In this paper we describe new mixed supramolecular adducts obtained by self-aggregation of two monomers, one containing the bioactive peptide and the other containing a chelating agent able to complex the gadolinium ion. By using these monomers, the gadolinium/octreotide ratio can be modulated as well with the possibility of influencing the size and shape of the resulting supramolecular aggregates; we describe nanoparticles containing a large amount of gadolinium complexes on the hydrophilic shell, while octreotide peptides are diluted on external aggregate surface. The assembling properties and the relaxometric behavior of the mixed aggregates are reported.

Materials and Methods

Protected N$^{\alpha}$-Fmoc-amino acid derivatives, coupling reagents, H-Thr(*t*Bu)-ol-(2-chloro-trityl)-resin and Rink amide MBHA resin were purchased from Calbiochem-Novabiochem (Laüfelfingen, Switzerland). The Fmoc-AdOO-OH was from Neosystem (Strasbourg, France). The DTPAGlu(*t*Bu)$_5$ and *N*,*N*-dioctadecylsuccinamic acid were prepared according to experimental procedures reported in Ref. 27,28. (DOTA(*t*Bu)$_3$ and (DTPA(*t*Bu)$_4$ were purchased from Macrocycles (Dallas TX USA). All other chemicals were commercially available by Sigma-Aldrich (Bucks, Switzerland) or LabScan (Stillorgan, Dublin, Ireland) and were used as received unless otherwise stated. All solutions were prepared by weight with doubly distilled water. Solid phase peptide synthesis was performed on a 433A Applied Biosystems automatic synthesizer (Carlsbad, California). Analytical RP-HPLC runs were carried out on an HP Agilent Series 1100 apparatus (Agilent, Santa Clara, CA, USA) using a Phenomenex (Torrance, CA) C18 column, 4.6 × 250 mm with a flow rate of 1.0 ml min^{-1}. For all the RP-HPLC procedures the system solvent used was 0.1% TFA in water (A) and 0.1% TFA in CH_3CN (B). The column was eluted with two linear gradients at 1.0 ml min^{-1} flow rate: (i) from 5 to 70% B in 30 min followed by 70 to 95% B in 10 min and (ii) from 60 to 80% B over 10 min and from 80 to 95% B over 15 min. Preparative RP-HPLC were carried out on a Shimadzu 8A (Kyoto, Japan) apparatus equipped with an UV Shimadzu detector using a Phenomenex C4 column, 22 × 250 mm with a flow rate of 20 ml min^{-1}, eluted with a linear gradient of 0.1% TFA in water (A) and 0.1% TFA in CH_3CN (B) as described above at 20 ml min^{-1} flow rate. Mass spectral analysis were carried out on MALDI-TOF Voyager-DE mass spectrometer Perseptive Biosystems (Framigham, MA, USA), and LC-MS analyses were performed by using Finnigan Surveyor MSQ single quadrupole electrospray ionization (Finnigan/Thermo Electron Corporation San Jose, CA, USA). ^{1}H and ^{13}C NMR spectra were recorded by using 400 spectrometer Varian (Palo Alto, CA, USA). UV measurements were performed on a UV-vis Jasco V-5505 spectrophotometer (Easton, MD) equipped with a Jasco ETC-505T Peltier temperature controller with a 1-cm quartz cuvette (Hellma).

Peptide Conjugate Synthesis

Peptide synthesis was carried out in solid-phase under standard conditions using Fmoc strategy on H-Thr(*t*Bu)-ol-(2-chrolotrityl)-resin (0.70 mmol g^{-1}, 0.15 mmol scale, and 0.214 g). The peptide chain was elongated by sequential coupling and Fmoc deprotection of the Fmoc-amino acid derivatives: Fmoc-Cys(Acm)-OH, Fmoc-Thr(O*t*Bu)-OH, Fmoc-Lys(Boc)-OH, Fmoc-D-Trp(Boc)-OH, Fmoc-Phe-OH, Fmoc-Cys(Acm)-OH, and Fmoc-D-Phe-OH. All couplings were performed twice for 1 h by using an excess of 4 equiv for the single amino acid derivatives. The Fmoc-amino acids were activated *in situ* by the standard HOBt/PyBop/DIEA procedure with DMF as solvent. Fmoc deprotection was carried out by 30% piperidine in DMF after each coupling step. The coupling steps were monitored by the qualitative Kaiser test. After completion of the synthesis of $(C_{18}H_{37})_2$-CONH(AdOO)$_5$-Octreotide ((C18)$_2$L5-Oct), the *N*-terminal Fmoc group was removed and five residues of

Fmoc-8-amino-3,6-dioxaoctanoic acid; HOBt, 1-hydroxy-1,2,3-benzotriazole; ICP, inductively coupled plasma; MRI, magnetic resonance imaging; Oct, octreotide; PET, positron emission tomography; PyBOP, benzotriazol-1-yl-oxytripyrrolidinophosphonium hexafluorophosphate; SANS, small angle neutron scattering, SPECT, single photon emission computed tomography; SPPS, solid phase peptide synthesis; SSTR, somatostatin receptor; TFA, trifluoroacetic acid.

Fmoc-AdOO-OH were sequentially added. These were coupled to the *N*-terminal amino group of D-Phe in successive single coupling step. An excess of 2 equiv of Fmoc-AdOO-OH, PyBop and HOBt, and 4 equiv of DIEA were dissolved in DMF and added to the manual vessel. When all five linkers were incorporated into the peptide chain, the *N,N*-dioctadecylsuccinamic acid was coupled using 4 equiv (2.48 g, 4.0 mmol) of the lipophylic compound dissolved in 10 ml of DMF/CH_2Cl_2 (50/50). Then 2.08 g (4.0 mmol) of PyBop, 0.61 g (4.0 mmol) of HOBt, and 1.34 ml (8.0 mmol) of DIEA, dissolved in DMF, were addedto the vessel as activating agents. The coupling time was 1 h under a N_2 stream at room temperature. Yield for aliphatic acid coupling, monitored by the Kaiser test, was in the range 95–98%. The deprotection (Acm removal) and the oxidation of the cysteine residues were carried out adding 1.2 equiv $Tl(CF_3CO_2)_3$ to a suspension of the peptidyl resin in DMF/anisole (19 : 1). The reaction mixture was stirred for 18 h at 0 °C and the progress was monitored at intervals by the colorimetric Ellmann test [29]. The peptide derivatives were cleaved from the solid support by suspending the resin in 10 ml TFA/TIS/H_2O (95.5/2/2.5) for 120 min. Free peptide derivatives were precipitated in cold water and lyophilized from a 50% H_2O/CH_3CN solution. The crude compounds were purified by preparative RP-HPLC. The single peaks were analyzed by HPLC and MS. Mass spectral analysis was carried out on MALDI-TOF. The desired compounds (∼180 mg) were obtained at HPLC purity higher than 95% and in a final yield of around 10%.

$(C_{18}H_{37})_2$-CONH(AdOO)$_5$-Octreotide, $(C18)_2$L5-Octreotide, *Rt* = 38.0 min; MW = 2328 amu

Synthesis of $(C_{18}H_{37})_2$CONHLys-(DOTA)CONH$_2$ $(C18)_2$DOTA, $(C_{18}H_{37})_2$CONHLys-(DTPA)CONH$_2$ $(C18)_2$DTPA, and $(C_{18}H_{37})_2$CONHLys-(DTPAGlu)CONH$_2$ $(C18)_2$DTPAGlu

$(C18)_2$DTPAGlu, (C18)2DTPA, and $(C18)_2$DOTA monomers were synthesized on solid support under standard conditions using Fmoc strategy, as reported elsewhere, [25]. The cleavage from the resin and deprotection of the *t*Bu protecting groups were performed in 10 ml of TFA/TIS/H_2O (95.5/2/2.5) for 120 min. The crude products were washed several times with small portions of cold water and lyophilized. The white solids were recrystalized from MeOH/H_2O and recovered in high yield (>85%). The products were characterized by mass spectra (electrospray ionization ESI) and NMR spectroscopy.

$(C18)_2$DOTA: MS (ESI^+): m/z (%): 1134 (100) [M-H^+]
$(C18)_2$DTPA: MS (ESI^+): m/z (%): 1123 (100) [M-H^+]
$(C18)_2$DTPAGlu: MS (ESI^+): m/z (%): 1195 (100) [M-H^+]

$(C18)_2$DTPAGlu. ^{1}H-NMR ($CDCl_3$/CD_3OD 50/50) (chemical shifts in δ, $CHCl_3$ as internal standard 7.26) = 4.1 (m, 1H, αCH Lys), 3.5 (overlapped, 1H, αCH Glu), 3.3 (s, 8H, NCH_2COOH), 2.7–2.8 (m, 8H, RNCH_2CH_2NR), 2.14 (m 2H, C(O)$CH_2$$CH_2$R), 1.87 (m, γ CH_2 Lys), 1.76 (m, 2H, δ CH_2 Lys), 1.65 (m, 2H, β CH_2 Lys), 1.5 (overlapped, 2H, R$CH_2$$CH_3$), 1.1–1.3 (m, 30 H, 15 CH_2), δ 0.8 (t, 3H, 1 CH_3).

^{13}C-NMR ($CDCl_3$/CD_3OD 50/50) (chemical shifts in δ, $CDCl_3$ as internal standard 77.00) = 176.2 (5, CO), 172.1 (2, CONH), 163.4 (2, CONH), 55.4 (NHCH(CH_2CH_2COOH)CO)55.04 (CH_2COOH), 54.61 (NH$(CH_2)_4$CH), 52.91 (NCH_2CH_2N), 49.7 ($CH_3(CH_2)_{16}CH_2$N), 46.4 ($CH_3(CH_2)_{15}CH_2CH_2$N), 38.0 (NHC$H_2(CH_2)_2CH_2$CH), 36.0 (NH$(CH_2)_3CH_2$CH), 33.0 (NCOCH_2CH_2CONH), 32.1 (NHCH(CH_2COOH)CO), 32.0 (NCOCH_2CH_2CONH), 31.8 (NHC$H_2CH_2$$(CH_2)_2$CH), 29.6-26.8 ($CH_3CH_2CH_2(CH_2)_{13}CH_2CH_2$N), (NHCH($CH_2$$CH_2$COOH)CO), 22.57 ($CH_3CH_2CH_2(CH_2)_{15}$), 22.18 (NH$(CH_2)_2CH_2$$CH_2$CH), 13.65 ($CH_3CH_2(CH_2)_{16}$).

$(C18)_2$DTPA. ^{1}H-NMR ($CDCl_3$/CD_3OD 50/50) (chemical shifts in δ, $CHCl_3$ as internal standard 7.26) = 4.3 (m, 1H, C*H* Lys α, m, 2H, R_2NCH_2CONHR), 3.6 (s, 8H, R_2NCH_2COOH), 3.44 (m, 4H, R_2N-CH_2CH_2N R_2), 3.30-3.27 (m, 4H, N-C*H*2), 3.19 (m, 4H, R_2N-CH_2CH_2NR_2), 3.1(m 2H, CH_2 Lys ε), 2.6-2.3 (m, 4H, NHCOCH_2CH_2CO), 1.90 (m, 2H, CH_2 Lys β), 1.6 (m, 2H, CH_2 Lys δ), 1.45 (m, 2H, CH_2 Lys γ), 1.4 (m, 4H, RCH_2CH_2N), 1.27 (m, 60 CH_2 aliphatic), 0.89 (t, 6H, CH_3).

^{13}C-NMR ($CDCl_3$/CD_3OD 50/50) (chemical shifts in δ, $CDCl_3$ as internal standard 77.00) = 173.31 (4, CO), 172.1 (2, CONH), 163.4 (2, CONH), 55.04 (CH_2COOH), 54.51 (NH$(CH_2)_4$CH), 52.91 (NCH_2CH_2N), 49.7 ($CH_3(CH_2)_{16}CH_2$N), 46.4 ($CH_3(CH_2)_{15}CH_2CH_2$N), 38.0 (NHC$H_2(CH_2)_2CH_2$CH), 36.0 (NH$(CH_2)_3CH_2$CH), 32.0 (NCOCH_2CH_2CONH), 31.8 (NHC$H_2CH_2$$(CH_2)_2$CH), 29.6-27.0 ($CH_3CH_2CH_2(CH_2)_{13}CH_2CH_2$N), 22.57 ($CH_3CH_2CH_2(CH_2)_{15}$), 22.18 (NH$(CH_2)_2CH_2CH_2$CH), 13.73 ($CH_3CH_2(CH_2)_{16}$).

$(C18)_2$DOTA. ^{1}H-NMR ($CDCl_3$/CD_3OD 50/50) (chemical shifts in δ, $CHCl_3$ as internal standard 7.26) = 4.1 (m, 1H, C*H* Lys α), 3.6 (m, 2H, R_2NCH_2CONH), 3.1 (m, 6H, R_2N-CH_2COOH), 3.0 2H, CH_2 Lys ε), 3.1 (m, 16 R_2N-CH_2CH_2NR_2) 2.4-2.1 (m, 4H, COCH_2CH_2CO), 1.7 (m, 2H, CH_2 Lys β), 1.4 (m, 2H, CH_2 Lys δ), 1.3 (m, 2H, CH_2 Lys γ), 1.1 (m, 4H, RCH_2CH_2N), 1.0 (m, 60 CH_2 aliphatic), 0.70 (t, 6H, CH_3).

^{13}C-NMR ($CDCl_3$/CD_3OD 50/50) (chemical shifts in δ, $CDCl_3$ as internal standard 77.00) = 174.0 (3, *C*OOH), 172.8, 172.6, 172.1, 163.0 (4 CONH), 54.5 (*C*H-Lys α), 53.2 (CH_2COOH), 51.50 (NCH_2CH_2N), 49.7 ($CH_3(CH_2)_{16}CH_2$N), 46.4 ($CH_3(CH_2)_{15}CH_2$CH2N), 38.0 (CH_2-Lys ε), 36.0 (CH_2-Lys β), 32.0 (NCOCH2CH_2CONH), 31.8 (CH_2-Lys γ), 29.60-27.0 ($CH_3CH_2CH_2(CH_2)_{13}CH_2CH_2$N), 22.57 ($CH_3CH_2CH_2(CH_2)_{15}$), 22.2 ($CH_2$-Lys δ), 13.73 ($CH_3CH_2(CH_2)_{16}$).

Preparation of Gadolinium Complexes

Gadolinium complexes were obtained by adding light excesses of $GdCl_3$ to the aqueous solutions of ligands at neutral pH and room temperature. The excess of uncomplexed Gd(III) ions was removed by centrifugation of the solution brought to pH 10; xylenol orange test [30] was applied to assure complete removal of Gd(III) ions.

Aggregates Preparation

Self-assembling of $(C18)_2$DOTA, $(C18)_2$DTPA, and $(C18)_2$DTPAGlu into aggregates and of $(C18)_2$DTPAGlu/$(C18)_2$L5-Oct, $(C18)_2$DTPA/$(C18)_2$L5-Oct, and $(C18)_2$DOTA/$(C18)_2$L5-Oct (or their corresponding gadolinium complexes) into mixed aggregates was obtained by dissolving the amphiphiles in small amounts of MeOH/$CHCl_3$ (50/50) mixture and subsequent evaporation of the solvent by slow rotation of the tube containing the solution under a stream of nitrogen. In this way, a thin film of amphiphile was obtained. Then the film was hydrated by the addition of 0.1 M phosphate buffer, pH 7.4, 0.9% wt NaCl into the vial and sonication for 30 min. All mixed aggregates were prepared at 90/10 molar ratio of the chelating agent-containing monomer and the octreotide-containing monomer. The pH was controlled with a pHmeter MeterLab PHM 220 (Livermore, CA). Concentrations of solutions were determined spectroscopically using a molar extinction coefficient (ε_{280}) of 5630 M^{-1} cm^{-1} for octreotide with its Trp residue in the sequence [31,32]. In all solutions used for SANS investigations,

Journal of PeptideScience

H_2O has been replaced by D_2O in order to minimize the incoherent contribution to the total scattering cross section. The total concentration in the samples used in structural measurements are in the $2.0 \cdot 10^{-3}$ M range.

Fluorescence Measurements

The fluorescence emission spectra were recorded using a Jasco Model FP-750 spectrofluorimeter (Easton, MD) equipped with a Peltier temperature controller in 1.0-cm path length quartz cell at 25 °C. Equal excitation and emission bandwidths were used throughout the experiments, with a recording speed of 125 nm min^{-1} and automatic selection of the time constant. Trp emission spectra in 290–450 nm range were obtained exciting at 280 nm the micelle solutions at a peptide concentration of $1.0 \cdot 10^{-5}$ M.

Small-Angle Neutron Scattering (SANS)

SANS were performed at 25 °C with the KWS2 and V4 instruments located at the Heinz Meier Leibtnitz Source, (Garching, Germany) and at the Helmholtz Zentrum (Berlin, Germany), respectively, with a setup widely described elsewhere [25,33]. The investigated systems were contained in a closed quartz cell, in order to prevent solvent evaporation and were kept under measurements for the period required for ~2 million counts. The obtained raw data were then corrected for background and empty cell scattering. Detector efficiency corrections, radial average, and transformation to absolute scattering cross sections $d\Sigma/d\Omega$ were made with plexiglass or water as secondary standards [34].

Water Proton Relaxation Measurements

The proton $1/T_1$ NMRD profiles were measured over a continuum of magnetic field strength from 0.00024 to 0.47 T (corresponding to 0.01–20 MHz proton Larmor Frequency) on a Stelar Fast Field-Cycling relaxometer (Mede Pavia, Italy). This relaxometer works under complete computer control with an absolute uncertainty in $1/T_1$ of ±1%. Data points from 0.47 T (20 MHz) to 1.7 T (70 MHz) were added to the experimental NMRD profiles and were recorded on the Stelar Spinmaster spectrometer (Mede Pavia, Italy) with switchable field from 20 to 70 MHz, by means of the standard inversion-recovery technique (16 experiments, 2 scans). A typical 90° pulse width was 4 μs and the reproducibility of the T_1 data was ±0.5%. The temperature was kept at 25 °C with a Stelar VTC-91 airflow heater (Mede Pavia, Italy) equipped with a copper-constant thermocouple (uncertainty ±0.1 °C), respectively. Relaxivity data at 20 MHz were measured on both instruments.

^{17}O-NMR Water Relaxation Rate Measurements

The exchange lifetime of a metal-bound water molecule in a paramagnetic chelate may be accurately assessed by measuring the temperature dependence of the paramagnetic contribution to the water ^{17}O transverse relaxation rate (R^o_{2p}). Variable temperature ^{17}O NMR measurements were recorded on the Bruker EX-600 spectrometer (Bruker Biospin, Rheinstetten, Germany) equipped with a 5-mm probe, by using a D_2O external lock. Experimental settings were spectral width 10 000 Hz, 90° pulse (7 μs), acquisition time 10 ms, 1000 scans, and no sample spinning. Solutions containing 2.6% of ^{17}O isotope (Yeda, Israel) were used. The paramagnetic contribution to the transverse relaxation rates (R^o_{2p}) were calculated from the signal width at half-height [$\Delta\nu_{1/2}$ corrected for the diamagnetic contribution ($\Delta\nu_{1/2}{}^{dia}$) : $R^o_{2p} = \pi(\Delta\nu_{1/2} - \Delta\nu_{1/2}{}^{dia})$]. The temperature dependences of the diamagnetic contribution to the observed transverse relaxation rates were measured by using ^{17}O isotope-enriched pure water.

Results and Discussion

Monomers Design and Synthesis

The schematic representation of the synthetic monomers, both containing a hydrophobic and a hydrophilic moiety, used to formulate mixed aggregates is reported in Figure 1. The first monomer $(C_{18}H_{37})_2NCO(CH_2)_2CO(AdOO)_5$-Oct ($(C18)_2$L5-Oct) contains two C18 hydrophobic moieties bound to the *N*-terminus of the cyclic peptide octreotide, and spaced from the bioactive peptide by five units of dioxoethylene linkers. The second monomer $(C18)_2$DTPAGlu, $(C18)_2$DTPA, or $(C18)_2$DOTA, contains two C18 hydrophobic moieties bound, through a lysine residue, to different polyamino-polycarboxy ligands: DTPAGlu, DTPA, or DOTA. DTPA or its glutamic analog DPTAGlu belong to the branched class of chelating agents, while DOTA belongs to the macrocycle chelating agents. The gadolinium ion can be complexed by nine ligands. The three chelating agents provide a set of eight donor couples of electrons, thus leaving the ninth position free for water coordination and allowing water exchange in the gadolinium coordination sphere. They were selected to study the influence of the steric hindrance and of the residual charge in the hydrophilic shell on the aggregation behavior. In fact, the expected difference between the three chelating agents and the respective amphiphilic monomers, are essentially due to the number of charges. They have 5, 4, and 3 negative charges as free bases and 2, 1, and 0 as gadolinium complexes, respectively.

In the peptide monomer, in order to maintain an appropriate exposition of the peptide on the external aggregate surface, five units of 8-amino-3,6-dioxaoctanoic acid (AdOO) were introduced between the hydrophobic double-tails and the octreotide *N*-terminal residue. The AdOO linker was chosen both to increase the hydrophilicity of the head without changing the charge of the monomers and to reduce aggregate clearance through the reticulo-endothelial system (RES) [35]. Moreover, the number of linkers was selected according to biological results previously obtained with similar aggregates prepared from derivatized CCK8 [22] or 7-14-bombesin [25], in order to favor a good exposure of octreotide on the external aggregate surface. It is already known that chemical modification of the residue of the octreotide at the *N*-terminal D-Phe by hydrophilic or hydrophobic chain does not modify the peptide affinity toward the receptors [36].

In both monomers, two alkyl chains of 18 carbon atoms were chosen as hydrophobic moieties in order to obtain a structure similar to the membrane phospholipidic bilayer, thus avoiding hemolytic effects on the cells [37]. Moreover, the 18th carbon chains provide a sufficient number of Van der Waals interactions to obtain stable aggregates.

Amphiphilic monomers were synthesized by solid-phase methods according to standard SPPS protocols [38]. Two different polymeric supports were used for the synthesis: Rink Amide MBHA resin for the chelating agent monomers; preloaded 2-chloro-trityl resin for the peptide monomer. Preloaded H-Thr(*t*Bu)-ol-(2-chloro-trityl) polymeric resin allows to obtain the alcoholic function on the octreotide *C*-terminus. At the end of the monomer assembly, the acetamidomethyl protecting groups were removed from the

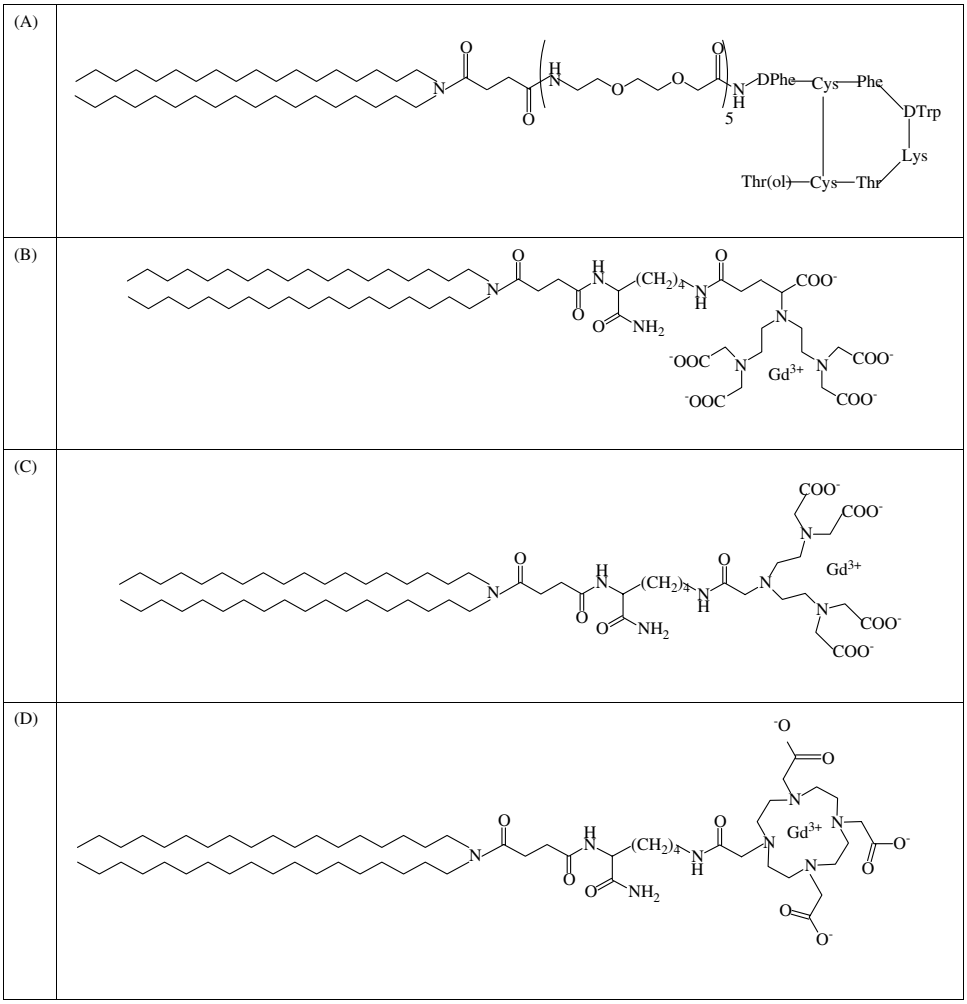

Figure 1. Schematic representation of amphiphilic monomers: (A) $(C_{18}H_{37})_2$N-CO$(CH_2)_2$CO-(AdOO)$_5$-Octreotide [(C18)$_2$L5-Oct]; (B) $(C_{18}H_{37})_2$N-CO$(CH_2)_2$CO-Lys(DTPAGlu-Gd)-NH$_2$ [(C18)$_2$DTPAGlu(Gd)]; (C) $(C_{18}H_{37})_2$N-CO$(CH_2)_2$CO-Lys(DTPA-Gd)-NH$_2$ [(C18)$_2$DTPA(Gd)]; (D) $(C_{18}H_{37})_2$N-CO$(CH_2)_2$CO-Lys(DOTA-Gd)-NH$_2$ (C18)$_2$DOTA(Gd). The amino acid sequence of octreotide is reported by using the three-letter code.

cysteine residues and disulfide bridge formation was achieved by $Tl(CF_3CO_2)_3$ treatment on the solid support. Monomer cleavages were performed using standard trifluoroacetic acid mixtures to allow for complete removal of all protecting groups of the amino acid side chains and of the *tert*-butyl groups from the carboxylic functions of the chelating agents. The crude products were purified by preparative reversed-phase HPLC or recrystallization to a final purity of 90% and were isolated in 30–40% yields in lyophilized form. Their molecular masses were determined by MALDI-TOF mass spectroscopy.

(C18)$_2$DTPAGlu(Gd), (C18)$_2$DTPA(Gd), and (C18)$_2$DOTA(Gd) gadolinium complexes were obtained by adding increasing amounts of a concentrated $GdCl_3$ solution to the free base monomers at neutral pH and at room temperature. To avoid the relaxivity contribution of free gadolinium, the excess metal ions were removed at pH 10 as insoluble hydroxide as already reported for other DTPA or DOTA like gadolinium complexes. The Gd(III) titration is conveniently followed by measuring ^{1}H-relaxation rates.

Self-assembling aggregates containing only the chelating agent monomers and mixed aggregates at 90/10 molar ratio between chelating agent monomer and peptide monomer were prepared by well-assessed sonication and extrusion procedures in 0.1 M phosphate buffer at pH 7.4 and physiological ionic conditions (0.9% wt). Larger amounts of peptide in the final composition of mixed aggregates were avoided in order to circumvent inter-chain peptide interaction and to preserve the right peptide conformation for the receptor binding. Peptide concentration in mixed aggregates was determined by UV spectroscopy. The exposure of the bioactive octreotide portion of the monomers on the surface of the aggregates was evaluated by monitoring the fluorescence of the of the tryptophan residue. Usually, this fluorophore shows an emission peak centered at 350 nm in polar solvents while in hydrophobic solvents the maximum is blue-shifted to 330 nm [39]. The fluorescence emission spectra of all aggregates (Figure 2) recorded at 25 °C and at a peptide concentration of 1.0×10^{-5} M show a maximum at ~340 nm. This is typical of a Trp of class II (about 340 nm) corresponding to the emission of this fluorophores contacting water molecules of low mobility at the protein surface [39].

Small-Angle Neutron Scattering

SANS measurements were performed on (C18)$_2$DTPAGlu/(C18)$_2$L5-Oct/D_2O, (C18)$_2$DTPA/(C18)$_2$L5-Oct/D_2O, and (C18)$_2$DOTA/(C18)$_2$L5-Oct/D_2O ternary systems, in which chelating agents are present as free bases or as gadolinium complexes. The

Journal of PeptideScience

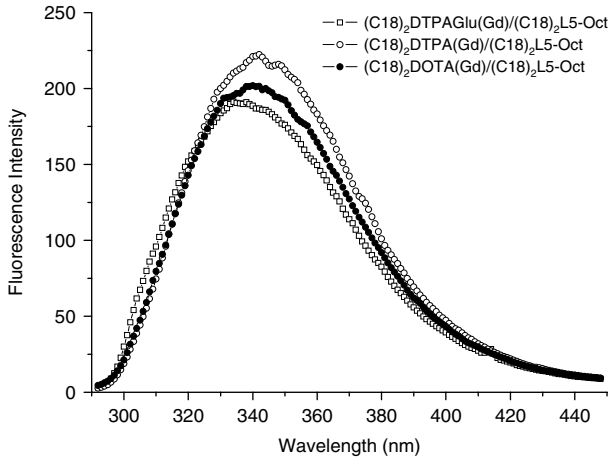

Figure 2. Fluorescence spectrum of tryptophan residue in $(C18)_2$DTPAGlu(Gd)/$(C18)_2$L5-Oct (□), $(C18)_2$DTPA(Gd)/$(C18)_2$L5-Oct (○), and $(C18)_2$DOTA(Gd)/$(C18)_2$L5-Oct (●) mixed aggregates. Peptide concentration in the samples was $1.0 \cdot 10^{-5}$ M. The spectrum was excited at 280 nm.

corresponding binary systems $(C18)_2$DTPAGlu-D_2O, $(C18)_2$DTPA-D_2O, and $(C18)_2$DOTA-D_2O have been also studied for comparison. The scattering profile of a sample containing only $(C18)_2$L5-Oct is quite flat, indicating that at this concentration solute aggregates are absent or in negligible amounts (data not shown).

Figure 3(A) and 3(B) shows the scattering cross section trend, $d\sum/d\Omega$ *versus* q, of the ternary and binary systems, respectively. Figure 3(A) shows that $(C18)_2$DTPAGlu/$(C18)_2$L5-Oct/D_2O and $(C18)_2$DTPAGlu(Gd)/$(C18)_2$L5-Oct/D_2O ternary systems show the typical form factor of small aggregates, i.e. spherical or ellipsoidal micelles. Indeed for the system containing Gd, a very small region in which a power law $d\Sigma/d\Omega \propto q^{-2}$, typical of two-dimensional objects, is present. Actually, as the Guinier region of liposomes and vesicles belongs to the USANS q range, these aggregates are seen, in the SANS domain as a collection of bilayers giving rise to the power law found. On the other hand, ternary systems based on DOTA chelating agents, as free base or as gadolinium complex, have scattering cross sections $d\Sigma/d\Omega$, scaling as q^{-2} typical of vesicles and liposomes, without any detectable presence of smaller aggregates. Finally, the ternary systems based on DTPA or DTPA (Gd) show the presence of a power law $d\Sigma/d\Omega \propto q^{-1}$ and $d\Sigma/d\Omega \propto q^{-2}$, respectively, indicating the presence of uni-dimensional objects like cylindrical micelles and the presence of vesicles, respectively.

Structural differences between the aggregates formulated by starting from the three chelating agents can be rationalized on the basis of their different number of carboxylic groups that at pH 7.4 are completely deprotonated. In fact, the negative charges diminish going from −5 for DTPAGlu to −4 for DTPA and −3 for DOTA. After their gadolinium complexation, −2, −1 and 0 negative charges remain for each DTPAGlu, DTPA, and DOTA, respectively. According to our previous findings, a reduction of the negative charges on these kinds of aggregates should promote a total or a partial micelle-to-vesicle transition. A decrease of negative charges in the surfactant head-group allows a decrease of the electrostatic repulsion between the head-groups, thus favoring the formation of large and low curvature aggregates such as bilayer structures or liposomes.

The ternary systems do not differ significantly from the respective binary systems (Figure 3(B)) except for the coexistence of micelles and vesicles for the systems containing the DTPAGlu molecule. The low difference can be ascribed to the relative low amount of the $(C18)_2$L5-Oct in mixed aggregates (10%) that probably does not influence in significant way the size and shape of the self-assembling aggregates.

Appropriate SANS models have been fitted to the experimental data by applying the appropriate form factor in dependence of the system analyzed, provided the solutions are quite dilute and inter-particle interactions are negligible. Systems containing two kinds of aggregates have been treated assuming each kind of aggregate scattered independently from the other and expressing the cross section as the sum of the form factors weighted for two scale factors depending on the relative density number of the objects and treating them as adjustable parameters.

Table 1 shows that the thicknesses of the bilayers are substantially constant, around 50 Å, in the analyzed systems.

Relaxivity Measurements

The key parameter for the evaluation of the efficiency of an MRI contrast agent is its relaxivity, i.e. the power to shorten the relaxation times of the solvent water protons. The measured relaxivity value ($r_{1\,p}$) is defined as the paramagnetic contribution to the measured proton longitudinal relaxation rate ($R_{1\,obs}$) of a solution containing 1.0 mM concentration of gadolinium complex according to Eqn (1) [40]

$$R_{1\,obs} = [GdL]r_{1\,p} + R_{1\,W} \quad (1)$$

where $R_{1\,w}$ is the diamagnetic contribution of pure water (0.38 s^{-1}). The relaxivity values determined (at 20 MHz and 25 °C) for the ternary systems are reported in Table 2. Moreover, relaxivity was measured as a function of the applied magnetic field to obtain the so-called NMRD (nuclear magnetic resonance dispersion) profiles reported in Figure 4. The Gd(III) concentration of all the measured samples was obtained by mineralization with HCl 37% at 120 °C overnight: from the measure of the observed relaxation rate ($R_{1\,obs}$) of the acidic solution, knowing the relaxivity ($r_{1\,p}$) of Gd(III) ion in acidic conditions (13.5 mM^{-1} s^{-1}), it was possible to calculate the exact Gd(III) concentration (Eqn (1)) (this method was calibrated using standard inductively coupled plasma (ICP) solutions, and the accuracy was determined to be 1%). At this point, knowing [GdL] and measuring $R_{1\,obs}$ of the micellar mother solution, the same Eqn (1) was used to calculate the micelle relaxivity.

NMRD profiles were measured on $(C18)_2$DTPAGlu(Gd)/$(C18)_2$L5-Oct/H_2O, $(C18)_2$DTPA(Gd)/$(C18)_2$L5-Oct/H_2O, and $(C18)_2$DOTA(Gd)/$(C18)_2$L5-Oct/H_2O ternary systems. The analysis of NMRD profiles of the lipophilic aggregated systems has been made according to the Solomon–Bloembergen–Morgan model, modified according to the Lipari–Szabo approach [41–43] to obtain an accurate determination of the reorientational correlation time (τ_R) that is strictly related to the molecular size of the investigated system. This model is generally applied to the systems with a faster local motion (governed by τ_l) and a slower global motion (governed by τ_g); the extent of local to global contribution to the overall motion is determined by an order parameter ($S2$) that can vary from 0 to 1. The experimental data reported in Figure 4 were fitted by considering one water molecule in the inner coordination sphere for each Gd(III) complex ($n_w = 1$) and a Gd-H distance of 3.1 Å.

Concerning reorientational correlation times (τ_g and τ_l), the global correlation times are quite similar in the case of the

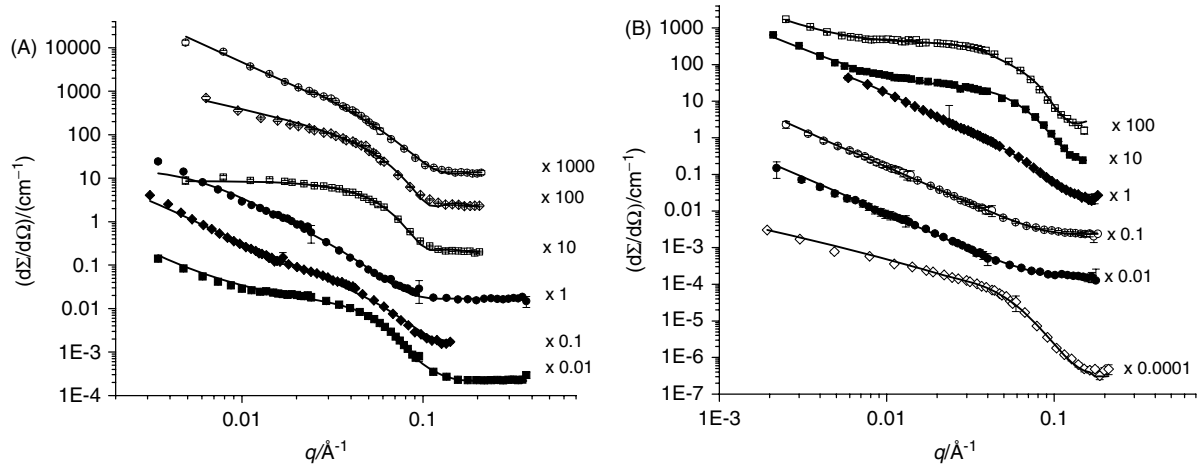

Figure 3. Scattering intensity profile for the following mixed systems at pH 7.4:

A

- ● $(C18)_2$DOTA(Gd)/$(C18)_2$L5-Oct
- ♦ $(C18)_2$DTPA(Gd)/$(C18)_2$L5-Oct
- ■ $(C18)_2$DTPAGlu(Gd)/$(C18)_2$L5-Oct
- ○ $(C18)_2$DOTA/$(C18)_2$L5-Oct
- ◊ $(C18)_2$DTPA/$(C18)_2$L5-Oct
- □ $(C18)_2$DTPAGlu/$(C18)_2$L5-Oct

B

- ● $(C18)_2$DOTA(Gd)
- ♦ $(C18)_2$DTPA(Gd)
- ■ $(C18)_2$DTPAGlu(Gd)
- ○ $(C18)_2$DOTA
- ◊ $(C18)_2$DTPA
- □ $(C18)_2$DTPAGlu

The solid line represents the fitting curve to the experimental data through the model reported in the text. For a better comparison, cross sections have been multiplied for a scale factor.

Table 1. Liposomal bilayer thickness (*d*) obtained for the systems investigated by means of SANS. The table also reports the radius of cylindrical micelles and the radius of spherical micelles, where found

Aqueous system	*d*/(´Å)	R_{cyl}/(´Å)	R_{sph}/(´Å)
$(C18)_2$DOTA(Gd)/D_2O	45 ± 4	–	–
$(C18)_2$DOTA/D_2O	41 ± 2	–	–
$(C18)_2$DTPA(Gd)/D_2O	50 ± 5	–	–
$(C18)_2$DTPA/D_2O	–	33 ± 3	–
$(C18)_2$DTPAGlu(Gd)/D_2O	72 ± 9	–	–
$(C18)_2$DTPAGlu/D_2O	53 ± 8	–	–
$(C18)_2$DOTA(Gd)/$(C18)_2$L5-Oct/D_2O	53 ± 2	–	–
$(C18)_2$DTPA(Gd)/$(C18)_2$L5-Oct/D_2O	51 ± 3	–	–
$(C18)_2$DTPAGlu(Gd)/$(C18)_2$L5-Oct/D_2O	49 ± 3	–	21 ± 2
$(C18)_2$DTPAGlu/$(C18)_2$L5-Oct/D_2O	–	–	20 ± 2
$(C18)_2$DTPA/$(C18)_2$L5-Oct/D_2O	–	28 ± 7	–
$(C18)_2$DOTA/$(C18)_2$L5-Oct/D_2O	50 ± 3	–	

micellar ternary systems containing $(C18)_2$DTPAGlu(Gd) and $(C18)_2$DTPA(Gd), while a consistently higher τ_g value has been found in the case of the bigger vescicular system containing $(C18)_2$DOTA(Gd). Quite surprisingly, a drop in the local correlation time (τ_l) going from $(C18)_2$DTPAGlu(Gd) to $(C18)_2$DTPA(Gd) and $(C18)_2$DOTA(Gd) containing systems has been found. For the $(C18)_2$DTPAGlu(Gd)/$(C18)_2$L5-Oct/H_2O mixed aggregate a set of parameters very close to the one of the corresponding to the ternary aggregate with CCK8 peptide [22] was observed.

One of the key parameters governing the relaxivity of a Gd-based contrast agent is the exchange lifetime of the water molecule coordinated to the metal ion (τ_M); this parameter is usually best determined by measuring the temperature dependence of the transverse relaxation rate of the ^{17}O water resonance. The exchange lifetime of $(C18)_2$DTPAGlu(Gd) has been previously determined and reported [22]. On the other hand, the direct ^{17}O-NMR R_{2p} *versus* T measurements were performed in the case of $(C18)_2$DTPA(Gd) (Table 2), while the low solubility of the $(C18)_2$DOTA(Gd) system prevented any direct ^{17}O-NMR measure and the τ_M value was left free to fit during the NMRD quantitative analysis. As expected on the basis of previously reported results [44,45], the water exchange lifetimes of the mono amides such as $(C18)_2$DTPA(Gd) and $(C18)_2$DOTA(Gd) are consistently slower than the one relative to $(C18)_2$DTPAGlu(Gd). From inspection of the Table 2, a decreasing trend in relaxivity values was observed going from $(C18)_2$DTPAGlu(Gd) to $(C18)_2$DTPA(Gd) to $(C18)_2$DOTA(Gd) containing ternary systems.

This phenomena can be well explained by a comparative analysis of relaxometric parameters. It is strictly related to the increase in the corresponding coordinated water exchange lifetimes (τ_M) which, for high molecular weight slowly moving systems, is known to be a limiting factor for values higher than 30–50 ns.

Conclusions

Supramolecular aggregates containing a high number of paramagnetic gadolinium complexes on their hydrophilic shell have been developed. They present high relaxivity values typical of the new generation of MRI contrast agents, based on nanoparticles obtained by lipophilic Gd(III) complexes. [46,47]. The presence of a small amount of amphiphilic octreotide monomer exposed on the aggregate surface gives the entire nanoparticles a potential binding selectivity toward somatostatin sstr2 receptor subtype. Structural differences between the aggregates formulated by starting from the three chelating agents, or from their gadolinium complexes, have been observed and rationalized on the basis of

Journal of PeptideScience

Table 2. Principal relaxometric parameters measured at pH 7.4, T = 298 K as derived from the fitting of NMRD (τ_R, Δ^2, τ_V) and ^{17}O-NMR (τ_M) data

Systems	$r_{1\,p}$ ($mM^{-1}\,s^{-1}$)	τ_I (ps)	τ_g (ps)	S	τ_M (ns)	τ_v (ps)	Δ^2 ($\times 10^{19}\,s^{-2}$)
$(C18)_2$DTPAGlu(Gd)/$(C18)_2$L5-Oct	17.6	302	2546	0.41	81	49.2	1.18
$(C18)_2$DTPA(Gd)/$(C18)_2$L5-Oct	15.2	63.5	2111	0.49	205	56.2	0.83
$(C18)_2$DOTA(Gd)/$(C18)_2$L5-Oct	10.0	65.5	3434	0.34	750	47.5	0.79

For fitting of NMRD profiles, Gd-H distance of the inner sphere water molecule was fixed to 3.1 Å, the distance of closest approach of outer sphere water molecules was fixed to 3.8 Å and the diffusion coefficient of the water molecules was fixed to 2.24×10^{-5} $cm^2\,s^{-1}$.

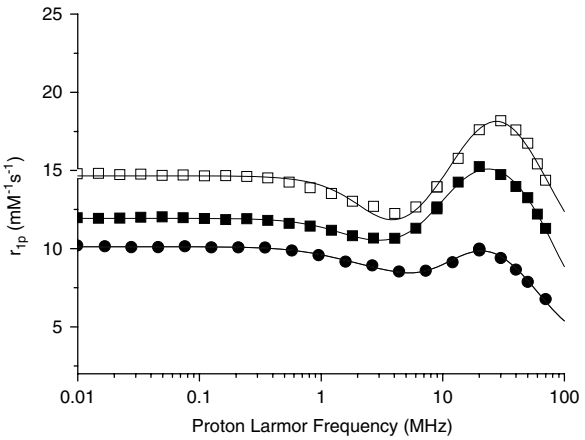

Figure 4. 1/T1 profiles of NMRD of $(C18)_2$DTPAGlu(Gd)/$(C18)_2$L5-Oct (□), $(C18)_2$DTPA(Gd)/$(C18)_2$L5-Oct (■), and $(C18)_2$DOTA(Gd)/$(C18)_2$L5-Oct (●) at pH 7.4 and 298 K, normalized to 1 mM concentration of Gd(III) ion, as function of frequency (MHz). The solid curves through the data points were calculated with the parameters reported in Table 2. Relaxivity parameters, reported in Table 2, are measured at 20 MHz.

their different residual charge. According to other reported systems [39], a decrease of the negative charges on the aggregate surface diminishes the electrostatic repulsion between the headgroups, thus favoring the formation of large and low curvature aggregates such as bilayer structures or liposomes. This finding promotes a micelle-to-vesicle transition going from −2 for DTPAGlu(Gd) to −1 for DTPA(Gd) and 0 for DOTA(Gd). A decrease in relaxivity values (from $r_{1\,p} = 17.6$ to $10.0\,mM^{-1}\,s^{-1}$), due to an increase of water exchange lifetimes (τ_M) of the mono amides, was observed going from $(C18)_2$DTPAGlu(Gd) to $(C18)_2$DOTA(Gd) containing ternary systems.

References

1 Berthold M, Bartfai T. Modes of peptide binding in G Protein-Coupled Receptors. *Neurochem. Res.* 1997; **22**: 1023–1031.
2 Reubi JC. Peptide receptors as molecular targets for cancer diagnosis and therapy. *Endocr. Rev.* 2003; **24**: 389–427.
3 Lamberts SWJ. *Octreotide: The Next Decade*. Bioscientifica: UK, Bristol, UK, 1999.
4 Bauer W, Briner U, Doepfner W. SMS 201–995: a very potent and selective octapeptide analogue of somatostatin with prolonged action. *Life Sci.* 1982; **31**: 1133–1140.
5 Veber DF, Freidinger RM, Schwenk-Perlow D, Paleveda WJ Jr, Holly FW, Strachan RG, Nurr RF, Arison BH, Homnick C, Randall WC, Glitzer MS, Saperstein R, Hirschmann R. A potent cyclic hexapeptide analogue of somatostatin. *Nature* 1981; **292**: 55–58.
6 Patel CY. Somatostatin and its receptor family. *Front. Neuroendocrinol.* 1999; **20**: 157–198.
7 Hofland LJ. Internalization of [DOTA,125I-Tyr3]octreotide by somatostatin receptor-positive cells in vitro and in vivo: implications for somatostatin receptor-targeted radio-guided surgery. *Proc. Assoc. Am. Physicians* 1999; **111**: 63–69.
8 Huang CM, Wu YT, Chen ST. Targeting delivery of paclitaxel into tumor cells via somatostatin receptor endocytosis. *Chem. Biol.* 2000; **7**: 453–461.
9 Mier W, Eritja R, Ashour M, Haberkorn U, Eisenhut M. Peptide–PNA conjugates targeted transport of antisense therapeutics into tumours. *Angew. Chem. Int. Ed.* 2003; **42**: 1968–1971.
10 Lamberts SWJ, Krenning EP, Reubi JC. The role of somatostatin and its analogs in the diagnosis and treatment of tumors. *Endocr. Rev.* 1991; **12**: 450–482.
11 Krenning EP, Kwekkeboom DJ, Pauwels S, Kvols LK, Reubi JC. Somatostatin receptor scintigraphy. In *Nuclear Medicine Annual*, Freeman LM (ed.). Lippincott-Raven: New York, 1995; 1–50.
12 Reubi JC, Waser B, Schaer JC, Laissue JA. Somatostatin receptor sst1-sst5 expression in normal and neoplastic human tissues using receptor autoradiography with subtype-selective ligands. *Eur. J. Nucl. Med.* 2001; **28**: 836–846, Erratum in: *Eur. J. Nucl. Med.* 2001; **28**: 1433.
13 Froidevaux S, Eberle AN. Somatostatin analogues and radiopeptides in cancer therapy. *Biopolymers (Pept. Sci.)* 2002; **66**: 161–183.
14 Allen TM. Ligand-targeted therapeutics in anticancer therapy. *Nat. Rev. Cancer* 2002; **2**: 750–763.
15 Wu H, Chang D-K. Peptide-mediated liposomal drug delivery system targeting tumor blood vessels in anticancer therapy. *J. Oncol.* 2010; ASAP DOI 10.1155/2010/723798.
16 van Tilborg GAF, Mulder WJM, Deckers N, Storm G, Reutelingsperger CPM, Strijkers GJ, Nicolay K. Annexin A5-functionalized bimodal lipid-based contrast agents for the detection of apoptosis. *Bioconjug. Chem.* 2006; **17**: 741–749.
17 Mulder WJM, Strijkers GJ, van Tilborg GAF, Cormode DP, Fayad ZA, Nicolay K. Nanoparticulate assemblies of amphiphiles and diagnostically active materials for multimodality imaging. *Acc. Chem. Res.* 2009; **42**: 904–914.
18 Bull SR, Guler MO, Bras RE, Maede TJ, Stupp SI. Self-assembled peptide amphiphile nanofibers conjugated to MRI contrast agents. *Nano Lett.* 2005; **5**: 1–4.
19 Kluza E, van der Schaft DWJ, Hautvast PAI, Mulder WJM, Mayo KH, Griffioen AW, Strijkers GJ, Nicolay K. Synergistic targeting of $\alpha v\beta 3$ integrin and galectin-1 with heteromultivalent paramagnetic liposomes for combined MR imaging and treatment of angiogenesis. *Nano Lett.* 2010; **10**: 52–58.
20 Ferrari M. Cancer nanotechnology: opportunities and challenges. *Nat. Rev. Cancer* 2005; **5**: 161–171.
21 Accardo A, Tesauro D, Roscigno P, Gianolio E, Paduano L, D'Errico G, Pedone C, Morelli G. Physicochemical properties of mixed micellar aggregates containing CCK peptides and Gd complexes designed as tumor specific contrast agents in MRI. *J. Am. Chem. Soc.* 2004; **126**: 3097–3107.
22 Accardo A, Tesauro D, Morelli G, Gianolio E, Aime S, Vaccaro M, Mangiapia G, Paduano L, Schillén K. High-relaxivity supramolecular aggregates containing peptides and Gd complexes as contrast agents. *J. Biol. Inorg. Chem.* 2007; **12**: 267–276.
23 Vaccaro M, Mangiapia G, Paduano L, Gianolio E, Accardo A, Tesauro D, Morelli G. Structural and relaxometric characterization peptide aggregates containing gadolinium complexes as potential selective contrast agents in MRI. *ChemPhysChem* 2007; **8**: 2526–2538.

24 Tesauro D, Accardo A, Gianolio E, Paduano L, Teixeira J, Schillen K, Aime S, Morelli G. Peptide derivatized lamellar aggregates as target-specific MRI contrast agents. *ChemBioChem* 2007; **8**: 950–955.
25 Accardo A, Mansi R, Morisco A, Mangiapia G, Paduano L, Tesauro D, Radulescu A, Aurilio M, Aloj L, Arra C, Morelli G. Peptide modified nanocarriers for selective targeting of bombesin receptors. *Mol. Biosyst.* 2010; **6**: 878–887.
26 Morisco A, Accardo A, Gianolio E, Tesauro D, Benedetti E, Morelli G. Micelles derivatized with octreotide as potential target-selective contrast agents in MRI. *J. Pept. Sci.* 2009; **15**: 242–250.
27 Anelli PL, Fedeli F, Gazzotti O, Lattuada L, Lux G, Rebasti F. L-glutamic acid and L-lysine as useful building blocks for the preparation of bifunctional DTPA-like ligands. *Bioconjug. Chem.* 1999; **10**: 137–140.
28 Schmitt L, Dietrich C. Synthesis and characterization of chelator-lipids for reversible immobilization of engineered proteins at self-assembled lipid interfaces. *J. Am. Chem. Soc.* 1994; **116**: 8485–8491.
29 Ellmann GL. Tissue sulfhydryl groups. *Arch. Biochem. Biophys.* 1959; **82**: 70–77.
30 Brunisholz G, Randin M. The separation of the rare earths by ethylenediamine-tetraacetic acid (EDTA). IX. A cycle for the separation of the rare earths by fractionation. *Helv. Chim. Acta* 1959; **42**: 1927–1938.
31 Edelhoch H. Spectroscopic determination of tryptophan and tyrosine in proteins. *Biochemistry* 1967; **6**: 1948–1954.
32 Pace CN, Vajdos F, Fee L, Grimsley G, Gray T. How to measure and predict the molar absorption coefficient of a protein. *Protein Sci.* 1995; **4**: 2411–2423.
33 Vaccaro M, Accardo A, Tesauro D, Mangiapia G, Löf D, Schillen K, Soederman O, Morelli G, Paduano L. Supramolecular aggregates of amphiphilic gadolinium complexes as blood pool MRI/MRA contrast agents: physicochemical characterization. *Langmuir* 2006; **22**: 6635–6643.
34 Wignall GD, Bates FS. Absolute calibration of small-angle neutron scattering data. *J. Appl. Crystallogr.* 1987; **20**: 28–40.
35 Torchilin VP, Omelyanenko VG, Papisov MI, Bogdanov AJ, Trubetskoy VS, Herron JN, Gentry CA. Poly(ethylene glycol) on the liposome surface: on the mechanism of polymer-coated liposome longevity. *Biochim. Biophys. Acta* 1994; **119**: 11–20.
36 Wang Q, Graham K, Schauer T, Fietz T, Mohammed A, Liu X, Hoffend J, Haberkorn U, Eisenhut M, Mier W. Pharmacological properties of hydrophilic and lipophilic derivatives of octreotate. *Nucl. Med. Biol.* 2004; **31**: 21–30.
37 Anelli PL, Lattuada L, Lorusso V, Schneider M, Tournier H, Uggeri F. Mixed micelles containing lipophilic gadolinium complexes as MRA contrast agents. *Magn. Res. Mater. Phys. Biol. Med.* 2001; **12**: 114–120.
38 Chan WC, White PD. *Fmoc Solid Phase Peptide Synthesis*. Oxford University Press: New York, 2000.
39 Lackowicz JR. *Principles of Fluorescence Spectroscopy*. Plenum Press: New York, 1983.
40 Caravan P, Ellison JJ, McMurry TJ, Lauffer RB. Gadolinium(III) chelates as MRI contrast agents: structure, dynamics, and applications. *Chem. Rev.* 1999; **99**: 2293–2352.
41 Bloembergen N, Morgan LO. Proton relaxation times in paramagnetic solutions. Effects of electron spin relaxation. *J. Chem. Phys.* 1961; **34**: 842–850.
42 Lipari G, Szabo A. Model-free approach to the interpretation of nuclear magnetic resonance relaxation in macromolecules. 1. Theory and range of validity. *J. Am. Chem. Soc.* 1982; **104**: 4546–4559.
43 Lipari G, Szabo A. Model-free approach to the interpretation of nuclear magnetic resonance relaxation in macromolecules. 2. Analysis of experimental results. *J. Am. Chem. Soc.* 1982; **104**: 4559–4570.
44 Aime S, Botta M, Fasano M, Paoletti S, Terreno E. Relaxometric determination of the exchange rate of the coordinated water protons in a neutral Gd-III chelate. *Chem. Eur. J.* 1997; **3**: 1499–1504.
45 Powell DH, Favre M, Graeppi N, Dhubhghaill OMN, Pubanz D, Merbach AE. Solution kinetic behaviour of lanthanide (III) polyamino carboxylates from O-17 NMR-studies. *J. Alloys Compd.* 1995; **225**: 246–252.
46 Delli Castelli D, Gianolio E, Geninatti Crich S, Terreno E, Aime S. Metal containing nanosized systems for MR-molecular imaging applications. *Coord. Chem. Rev.* 2008; **252**: 2424–2443.
47 Accardo A, Tesauro D, Aloj L, Pedone C, Morelli G. Supramolecular aggregates containing lipophilic Gd(III) complexes as contrast agents in MRI. *Coord. Chem. Rev.* 2009; **253**: 2193–2213.

